



Numerical Analysis of Structures under The effect of Ground Shock Induced from Blast Loads

Tarek N. Salem¹/ Nabil M. Nagy²/ Ahmed Arafa³

ABSTRACT

Blast loads have come into attention in recent years due to the large number of accidental events. So, important and critical structures may be designed to resist transient extreme loads such as high velocity impacts and explosions. In reality, a surface explosion generates both ground shock and air blast pressure on nearby structures, of which the ground shock usually arrives at structure foundation earlier than air blast pressure because of the different wave propagation velocities in soil and air. The ground shock will excite the structure to move and it will not response to air blast pressure from zero initial condition. So, a separate study accounting for the effect of an explosion ground shock on a nearby structure has been performed using FEM software ABAQUS. The analysis started with a static step which include applying initial stress due to soil and structure's own weights, and additional structural loads, after that the model is analyzed under the blast loading near the structure, then a parametric study including the charge weight, the distance of the charge and the structure height has been performed. Results showed that the structure is exposed to additional displacements and deformations in both horizontal and vertical directions resulting in shifting its foundations and additional settlements.

Key words: Blast Load, Structural Response, Soil Behavior, ABAQUS.

1. INTRODUCTION

An explosion is defined by releasing a great amount of energy within a very short time period. This energy produces two main components; first is the air blast wave which spread out through the air and can cause damages to adjacent structures. The second part are the stress waves which spread out radially through the earth from the blast source causing ground vibrations which radiates out from the source with decreasing intensity and can excite the adjacent structures causing vibrations. These vibrations could reach sufficiently high levels which may damage the structures or cause additional internal forces in the structural elements. The energy travels in the form of waves, which may be illustrated by dropping a stone in a still pool of water. Near where the stone drops, waves are formed then spread concentrically out of the center. The waves have high amplitude at the drop point, but this magnitude decreases as the waves spread outwards, Lindsey [12].

The ground shock coming from an explosion usually arrives at a structure foundation earlier than air blast pressure because of the different wave propagation velocities in geomaterials and in the air, Wu and Hao [15]. Ground shock and air blast might act on the structure simultaneously, depending on the distance between the explosion center and the structure. Even though they do not act simultaneously, ground shock will excite the structure and the structure will not response to air blast pressure with zero initial condition.

More current practice usually considers only air blast pressure, and many empirical relations are available to predict air blast pressure, other studies were concerned with underground structures, military structures, tunnels, and pipelines, Kanarachos [11], Chowdhury [6], and Yang [17].

Few researches take only the effect of the ground shock on the structure foundation system, especially the shallow foundation and the blast effect on the bearing capacity of soil, Amini [2], and Gamber [9]. Other researches model the blast as an acceleration-time history affecting the structure foundations and do not take the soil properties into consideration, Xuansheng *et al.* [16]. The characteristics of an explosion stress waves are quite different from earthquake waves. The blast waves usually have high frequency, short time duration, equality of amplitudes in both horizontal and vertical directions, and large range of magnitudes from ten to thousands of the gravitational constant, Hossein [10].

Studies that discuss the effect of soil properties under blast loading are relatively few. Soil is an assembly of individual particles with varying constituents, sizes, voids ratio, and degree of saturation. The rapid release of energy from an explosive causes shockwave that propagates through the soil medium, An *et al.* [3]. The energy applied to a soil through external loads such as blast loads may both overcome the frictional resistance between the soil particles and also to expand the soil against the confining pressure. The soil grains are highly irregular in shape and have to be lifted over one another for sliding to occur, Darke and Little [7].

The mechanism of deformation in soil varies from cohesive saturated soil to dry soils. Deformations in cohesive soils can be divided into two types; (1) the soil skeleton deformation, (2) the deformation of all the soil phases. At high pressures, the soil skeleton deformation

¹ Professor, Faculty of Engineering, Zagazig University, Egypt, Email: nageeb2@yahoo.com

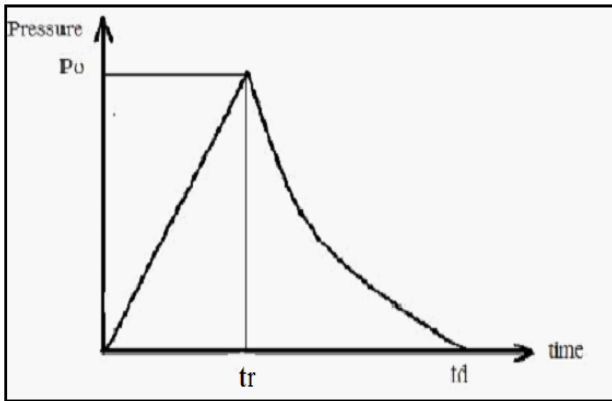
² Associate professor, Military Technical College, Cairo., Egypt, Email: nabilmnagy@yahoo.com

³ Graduate student, Faculty of Engineering, Zagazig University, Egypt, Email: stengahmedarfa2011@gmail.com

is given by the plastic deformation of bond and grain displacements. Volume compression of all soil phases plays a role in the deformation of all the soil phases, *Darina* [8]. In dry cohesive soil, deformation is dominated by particle linkage distortion and soil compaction. Tension is not considered as soil cannot bear large tensile stresses, *Barnes* [4]. Moreover, in dry soils at high pressures, grain bond distortion and soil compaction occur.

2. EXPLOSION PARAMETERS

When a blast occurs, the resulting internal stress and particle velocity of soil can be defined by exponential type time-histories. These values of stress and velocity quickly rise to a peak value and then exponentially decay to nearly zero over a very short period of time. The characteristic time for this time histories can be measured in arrival of from the source (t_a), where $t_a = R/c$, R is the distance from the explosion and c is the seismic or propagation velocity of the media. Typically



these wave forms rise sharply to the peak with the rise time (t_r), where $t_r = 0.10 t_a$, this is about 1/10 of the travel time to the target point. Figure (1) shows a typical time history diagram for pressure or velocity.

Figure (1) Typical Pressure Blast Time-History.

The peak values of free field stress and velocity, which are used in Equations (1) and (2), are given as,

$$P_0 = f \times \rho_c \times 160 \times \left(\frac{R}{W^{1/3}}\right)^{-n} \quad (1)$$

$$V_0 = f \times 160 \times \left(\frac{R}{W^{1/3}}\right)^{-n} \quad (2)$$

Where, P_0 : Peak stress (kPa), V_0 Peak particle velocity (m/sec.), ρ_c : Acoustic impedance (kPa/(m/sec)), R : Distance to the explosion (m), W : Charge weight (N), n : Attenuation coefficient, and f : Ground coupling factor which equals 0.4 for surface charge. The attenuation coefficient, seismic velocity and acoustic impedance can be estimated based on the soil type and properties. *Darke and Little* [7], *TM 5-855-1* [14], and *Bulson* [5] present ranges of values for these ground shock parameters based on measurements collected during various explosion tests.

3. NUMERICAL MODELING

Modeling is performed by *ABAQUS V 6.11* [1] software. Mohr-Coulomb model is used to represent the nonlinear soil behavior, with a linear elastic model used in modeling the concrete structure and its foundations.

3.1. Soil Model

The soil is modelled as dense sand with Mohr-Coulomb model parameters properties shown in Table (1). Mohr-Coulomb failure criteria is correct enough to reflect the soil behavior under blast load, *Gamber* [9]. The finite soil domain has dimensions of 100.0 m width and 40.0 m depth modelled with 10825 plane strain elements (CPE4R). The side boundaries are modeled with 130 infinite elements (CINPE4) with a dimension of 20.0 m length, these elements provide transmitting wave side boundaries in the dynamic analysis.

3.2. Structure Model

The structure is assumed to be made of reinforced concrete modelled with linear elastic properties, as presented in *Gamber* [9], and shown in Table (2). The structure consists of 10 stories with total height of 30.0 m and 5 bays with a total width of 20.0 m. The foundation is a raft with 1.0 m thickness resting directly on the soil. The columns and beams of the structure are modelled with 342 beam elements (B21) available in ABAQUS and have dimensions of 0.30×0.60 m. The raft is modelled with 80 plane strain elements (CPE4R). The foundation depth is assumed to be located at 1.0 m from the ground surface. Figure (2) shows the FEM model used in the analysis.

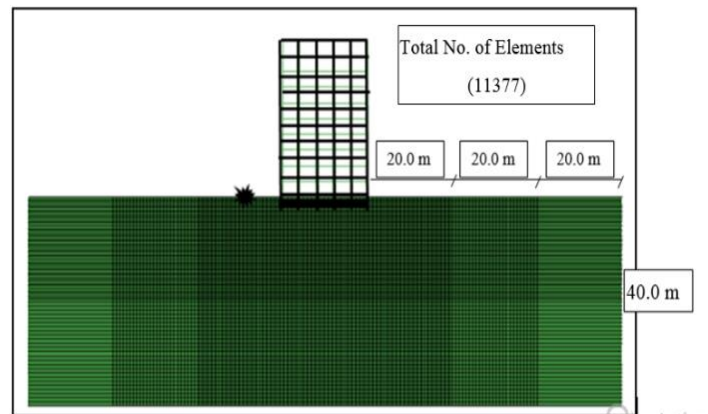


Figure (2) Finite Element Mesh of the Model.

The contact between the soil and foundation is needed here to capture the effect of uplift and sliding of the foundation over the subsoil during the dynamic effect of the blast ground shock. SSI is modelled with surface to surface contact in ABAQUS to model the interface between the soil and the foundation surface during the ground shock excitation. The mechanical properties of the contact surfaces defining the tangential and normal behavior of the contact surfaces can influence the results of the numerical simulation and should be chosen with great rigor. Normal behavior adopts "hard" contact in a pressure-over closure relationship, where a "hard" contact implies that the surfaces transmit no contact

pressure unless the nodes of one surface make contact with the other surface. The tangential behavior is modelled using a penalty method in which the friction coefficient is set equal to 0.60.

3.3. Loading Steps

At first, a geostatic step is used to generate the geo-stress of soil under its own weight with ramped amplitude over the duration of the step. After the initial conditions are established a static step is applied which includes applying the dead load of the structure and additional load of 15 kN/m' is applied as a line load over all the structure beams. These loads include the weight of slabs and live loads and are applied before the dynamic steps. The blast load with pressure for different charge weights in MPa assuming the same amplitude, as used by *Rosengren* [13] and shown in Figure (3) is applied in a dynamic step over the top soil boundary with at distance 5.0 m nearby the concrete structure. Table (3) shows the estimated explosion parameters for the charge used according to *Darke and Little* [7], with another dynamic step used after detonation of the explosion load to obtain the vibration of the structure resting on the subsoil.

Table 1.
Soil Parameters

| Property | Value |
|----------------------------------|-------|
| Unit weight (kN/m ³) | 19.00 |
| Young's modulus (Mpa) | 50 |
| Poisson ratio ν | 0.3 |
| Internal friction angle ϕ | 30° |

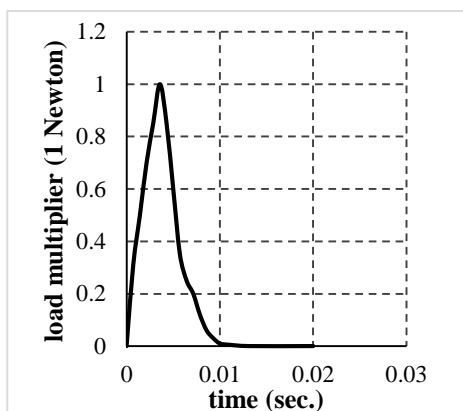


Figure (3) Blast Pressure Amplitude.

Table 3. Explosion Parameters.

| Property | Value |
|--|--------|
| Charge weight (N) | 162.3 |
| Acoustic impedance (ρ_c) Pa.sec/m | 1.0 E6 |
| Coupling factor | 0.4 |

4. PARAMETRIC STUDY AND ANALYSIS OF THE RESULTS

4.1. Effect of the Charge Distance (R)

The charge distance is the distance between the blast load and structure (R) is varied, and the used distances are 5.0 m, 7.0 m, 10.0 m and 15.0 m, and shown in the discussed results below.

4.1.1. Horizontal Displacements of the Structure

The leftmost point of foundation (nearest to the explosion location) is selected to observe the effect of

Table 2.
Concrete Parameters

| Property | Value |
|----------------------------------|-------|
| Unit weight (kN/m ³) | 24.00 |
| Young's modulus (GPa) | 22.9 |
| Poisson ratio | 0.15 |

charge distance on the displacements of foundations. It is found that increasing the charge distance resulted in reductions in the induced horizontal displacements of foundations, as shown in Figure (4).

The figure shows an instant spike reaching a maximum value just after the detonation followed by decaying oscillations around a horizontal displacement of about 0.017 m in case of 5.0 m standoff distance. The same trend is noticed for all the studied explosion distances but reaching lower spikes and oscillating around lower horizontal displacements, as shown in Figure (4).

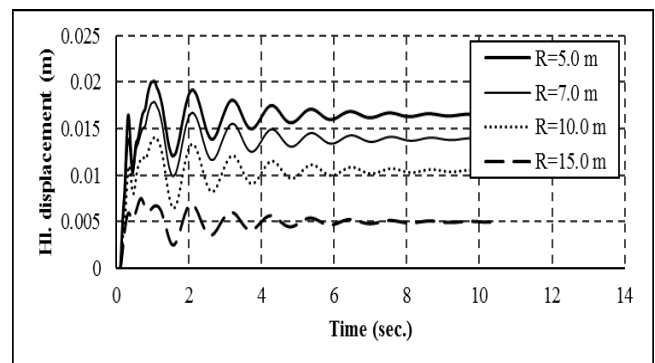


Figure (4) Horizontal Displacement of Foundation vs. Time for Different Charge Distances.

As shown in Figure (5), increasing the charge distance resulted in consistent reductions in the lateral response of the roof. The cyclic behavior of the upper left roof point is oscillating with much higher amplitude than the foundation same foundation point as shown in Figure (6). The same trend is noticed for all the studied explosion distances. The maximum horizontal displacement is about 8.20 cm, and oscillates at an average value of about 3.70 cm. Increasing the explosion position distance resulted in noticeable reductions in the induced lateral movements.

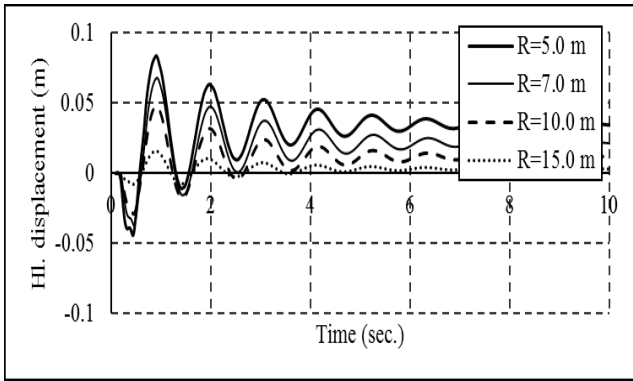


Figure (5) Horizontal Displacement of the Roof Point vs. Time for Different Charge Distances.

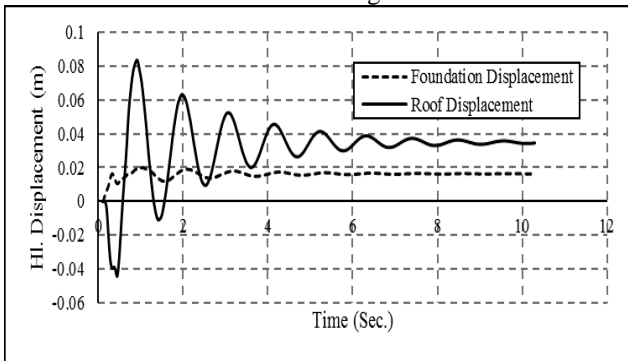


Figure (6) Horizontal Displacement of Structure Foundation and Roof Points at 5.0 m Charge Distance.

The maximum computed horizontal roof and foundation displacements are almost linearly decaying with increasing the distance from the detonation source, as shown in Figure (7) and presented in Equation (3) for foundations, and Equation (4) for the roof, as follows:

$$D_{HI, \max} = -0.0013 * R + 0.0266 \quad (3)$$

$$D_{HI, \max} = -0.0067 * R + 0.1156 \quad (4)$$

Where, D is the maximum horizontal displacement in (m), and R is charge distance in (m).

4.1.2. Vertical Displacements of the Structure

Figure (8) shows the maximum computed vertical displacement of leftmost foundation point as it is the most affected point of the structure regarding vertical movement. Starting from the computed settlements due to the structure loads for the static case, the explosion causes upward and downward movements with much less number of cycles than the horizontal movement. Moreover, the differences between the computed vertical movements of the foundations are much lower than the differences in the horizontal ones. In addition, slight permanent settlements are noticed at the end of the dynamic analysis period. Although the differences between the permanent settlements are small, but still the nearest distances resulted in the highest settlements and the lowest vertical heave.

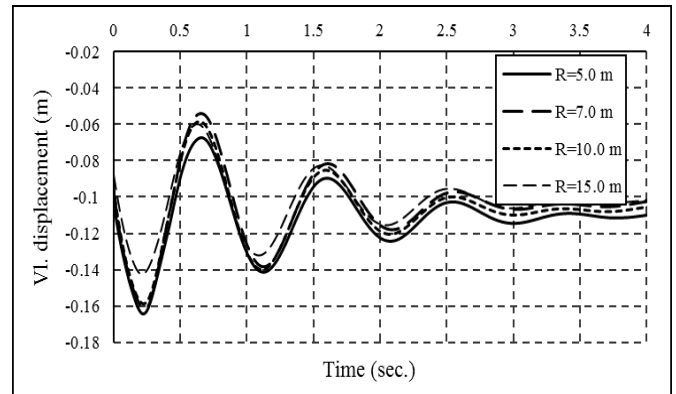


Figure (8) Vertical Displacement of Foundation Point vs. Time with Different Charge Locations.

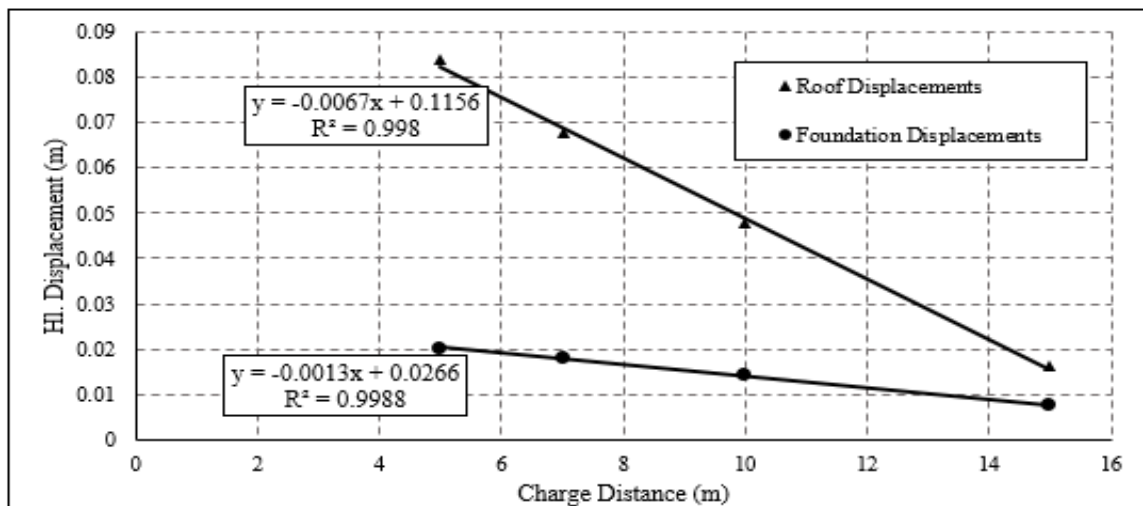


Figure (7) Maximum Horizontal Roof and Foundation Displacements of Structure vs. Charge Distance

When comparing the vertical displacements of the foundation point and the roof point it is observed that the two points have almost the same behavior of movement as shown in Figure (9) in all the studied cases. This is mainly due to the structure rigidity as it moves as a single block in the vertical direction.

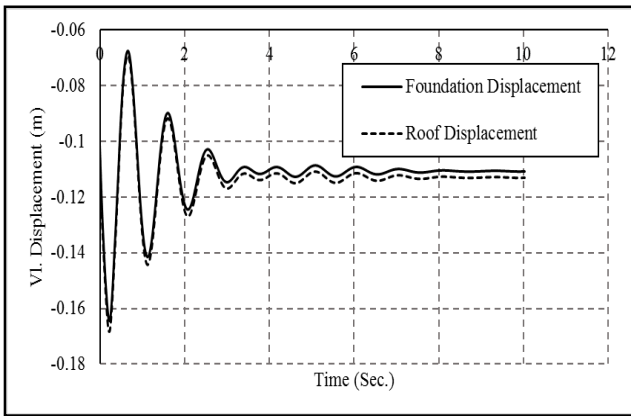


Figure (9) Vertical Displacement of Foundation and Roof Points vs. Time at 5.0 m Charge Distance.

4.2. Effect of The charge Weight (w)

4.2.1. Horizontal Displacements of Structures

The horizontal displacement of foundation is noticeably increased by increasing the charge weight especially at the roof point, which is roughly about 3.50 times the horizontal foundation displacements. The maximum response of this point is highlighted by a passing line presented in Equation (5) for the foundation displacements, and Equation (6) for the roof displacement, as shown in Figure (10).

$$D_{HI, \max (m)} = -1.0 * E^{-7} * W^2 + 0.0001 * W + 0.0003 \quad (5)$$

$$D_{HI, \max (cm)} = -7.0 * E^{-7} * W^2 + 0.0006 * W + 0.0035 \quad (6)$$

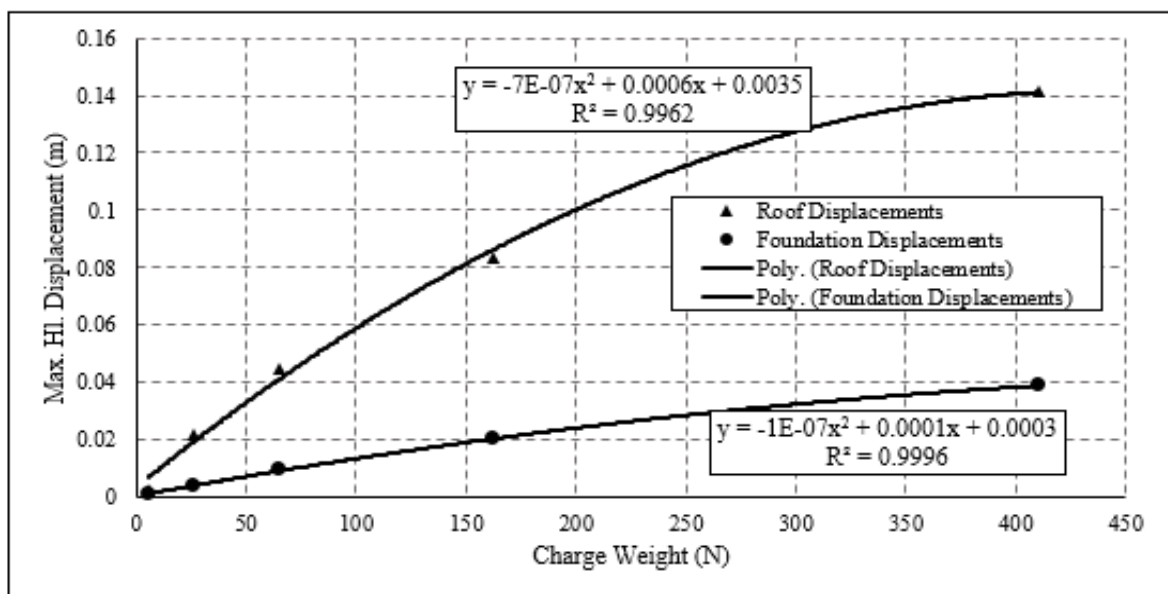


Figure (10) Maximum Horizontal Displacement vs. Different Charge Weights.

The maximum vibration response of the concrete frame structure is at the left roof point as shown in Figure (11). Higher charge weights resulted in higher horizontal displacement amplitudes. Moreover, much higher displacement amplitudes are computed at the structure roof than those computed at the foundation point, as shown in Figure (12).

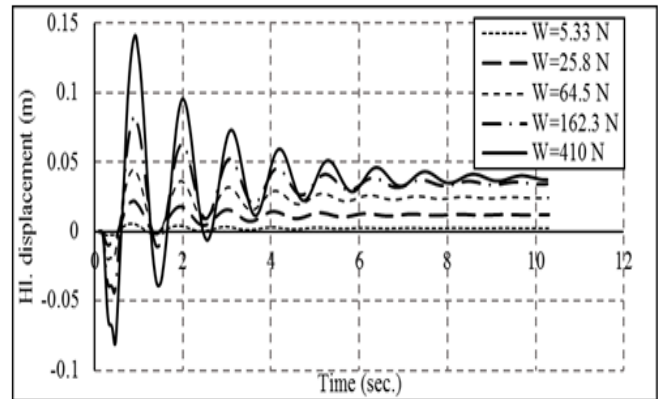


Figure (11) Horizontal Displacement of Roof Point vs. Time with Different Charge Weights.

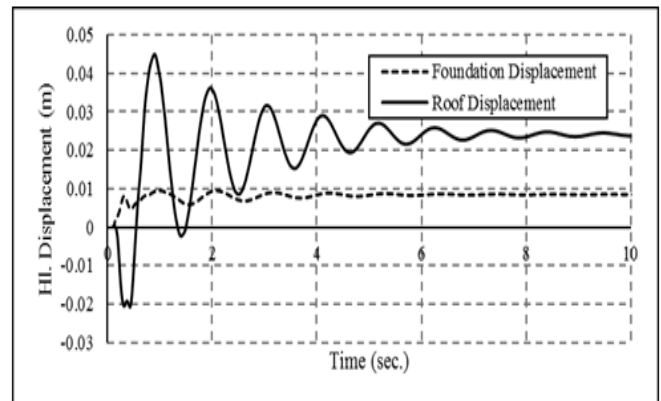


Figure (12) Horizontal Displacement of Structure vs. Time at 64.5 N Charge Weight.

4.2.2. Vertical Displacements of Structure

Figure (13) shows that increasing the charge weights resulted in slight increase in the amplitude of the vertical displacements generated explosion waves at the left foundation point. Moreover, slight permanent settlement took place after the blast shock wave action began to cease.

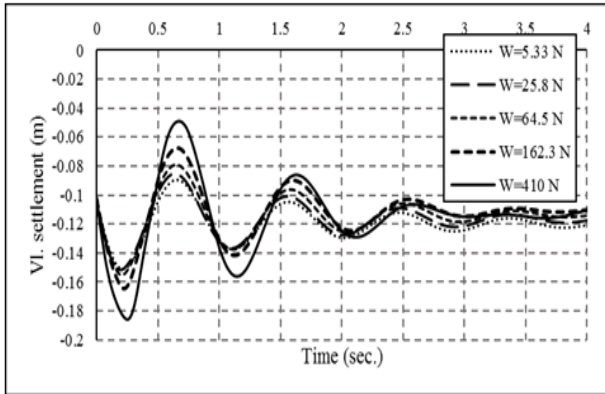


Figure (13) Vertical Displacement of Foundation Point vs. Time with Different Charge Weights.

4.3. Effect of Structure Height (H)

4.3.1. Horizontal Displacements of Structure

As the height of the structure increases, its weight also increases resulting in reducing the ability of the blast pressure to move the structure in the horizontal direction. A relation between the structure height and the maximum horizontal displacement of the foundation point is represented by Equation 7, and as shown in Figure (15).

$$D_{Hl. \max} (\text{cm}) = -7.0 * E^{-6} * H^2 - 2.0 * E^{-5} * H + 0.0272 \quad (7)$$

When comparing the horizontal displacements of the foundation point and the roof point it is observed that the maximum vibration response in all cases is at the roof point in the horizontal direction as shown in Figure (14). Increasing the structure height resulted in subsequent increase in the horizontal displacement increased at the roof point because of the flexibility of the structure increased as shown in Figure (15). On the other hand, increasing the structure height leads to increasing of vertical loads at the foundations which consequently causes less horizontal deformations at the foundations. A relation between the structure height and the maximum horizontal displacement of the foundations and roof points are represented by Equations (8) and (9) respectively:

$$D_{Hl. \max} (\text{cm}) = -7.0 * E^{-6} * H^2 - 2.0 * E^{-5} * H + 0.0272 \quad (8)$$

$$D_{Hl. \max} (\text{cm}) = -0.0002 * H^2 + 0.009 * H - 0.0485 \quad (9)$$

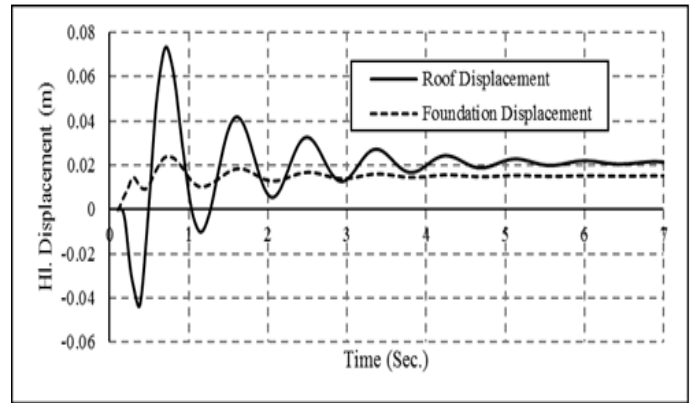


Figure (14) Horizontal Displacement of Structure vs. Time at 21.0 m Structure Height.

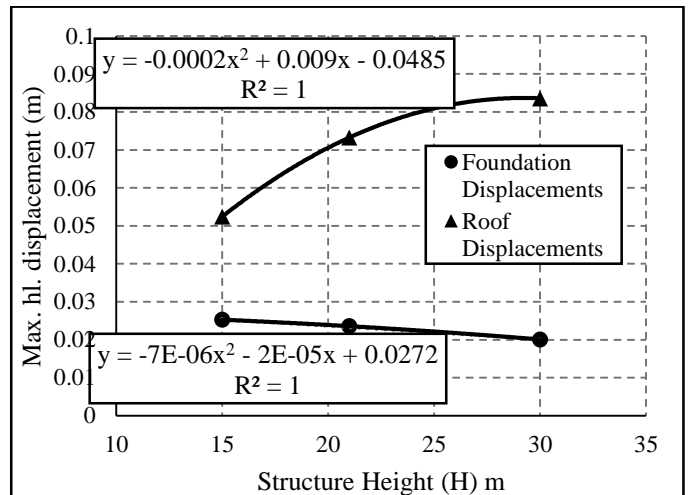


Figure (15) Maximum Horizontal Displacement of the structure vs. Structure Height.

4.3.2. Vertical Displacements of Foundation

Figure (16) shows the maximum vertical displacement of the leftmost foundation point as it is the most affected point of the structure. Increasing the structure height and consequently the structure weight resulted in increased settlements and amplitude of movement.

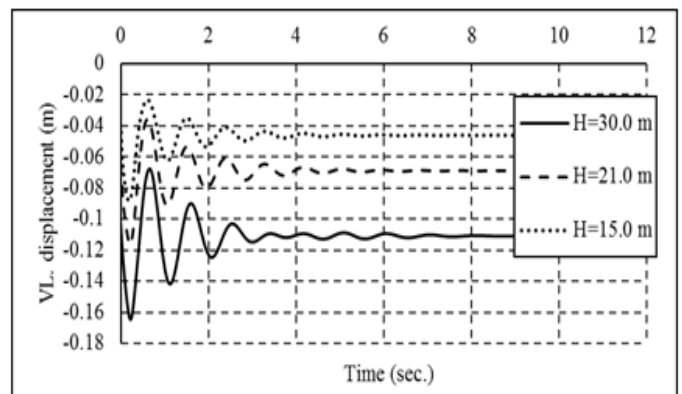


Figure (16) Vertical Displacement after Blast in Different Structure Height.

4.4. Effect of Soil Type

Soil types and properties including; modulus of deformation, Poisson's ratio, shear strength parameters have a great effect on the response of the structure under blast loads. Table (4) shows the properties used, the product of acoustic impedance and attenuation factor can be estimated for different soils based on the charts and figures provided by *Darke and Little* [7]. A 162.3 N charge weight is used in all the studied cases.

Table 4. Different Soil Parameters.

| Property | Unit weight (kN/m ³) | Young's modulus (MPa) | Poisson ratio ν | Cohesion (KPa) | Internal friction angle $^{\circ}$ | Acoustic impedance (ρ_c) Pa.sec/m | Friction coefficient |
|----------|----------------------------------|-----------------------|---------------------|----------------|------------------------------------|--|----------------------|
| Sand | 19.00 | 50.00 | 0.3 | --- | 30 $^{\circ}$ | 1.0E6 | 0.6 |
| Clay | 17.00 | 10.00 | 0.4 | 150 | --- | 0.25E6 | 0.5 |

4.4.1. Horizontal Displacements of Structures

The deformations and displacements of the structure is increased when decreasing the stiffness of the soil, with respect to the horizontal displacement of foundation it is the maximum for clay as 31.86 mm, and 20.0 mm in case of sand as shown in Figure (17). In addition, higher displacement amplitudes are noticed in the case of clay than those took place in sand, especially in the beginning of the explosion.

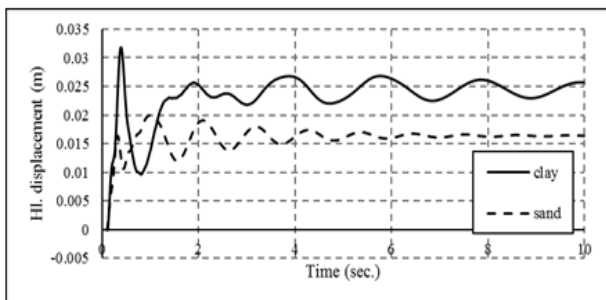


Figure (17) Horizontal Displacement of Foundation in Case of Clay and Sand.

As the maximum horizontal displacements took place at the roof, it is observed that the maximum lateral displacements are 115.0 and 80.0 mm in cases of clay and sand respectively, as shown in Figure (18).

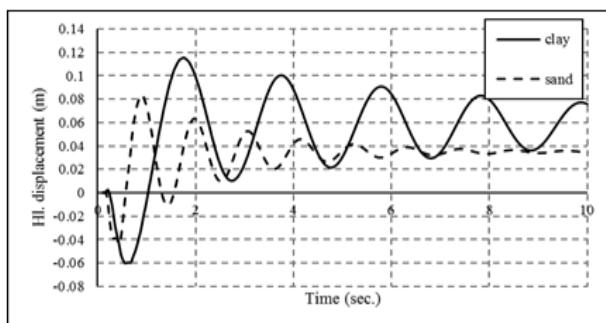


Figure (18) Horizontal Displacement of Roof in Case of Clay and Sand.

4.4.2. Vertical Displacements of Structures

The left point of foundation is selected as it was the most critical point in case of blast response. It should be noted that the starting values are the settlements that took in the soil due to the structure weight, as shown in Figure (19). Figure (19) shows that permanent relatively large settlements took place in clay due to the explosion, whereas the structure approximately returns to its original static position in case of sand soils.

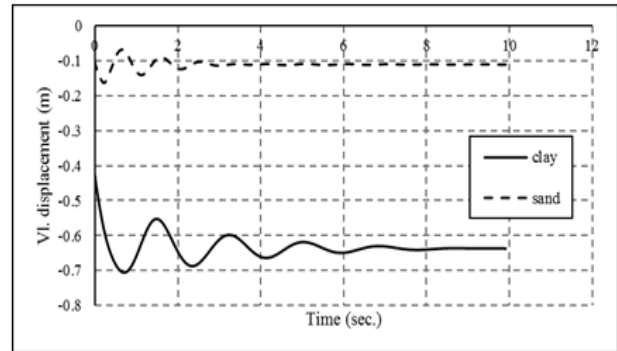


Figure (19) Vertical Displacement of Foundation in Case of Clay and Sand.

5. CONCLUSIONS

The performance of high-risk facilities such as public, commercial and industrial structures under extreme loads such as explosions and high velocity impact is an important problem. This study investigated the blast response of a multi-story concrete structure under blast loads with respect to blast waves travelling through the soils only. The structure is modeled as beam-column system. The blast load is modeled as a time-series of decaying amplitude. The soil is modelled with the Mohr-Coulomb constitutive model. Blasting can cause significant vibrations within structures even in cases where the blast source is far from the structure is. These conclusions are drawn from the current research:

- 1- In case of variation of charge distance; the response of structure is less pronounced when increasing the charge distance in both horizontal and vertical directions:
 - The maximum horizontal base displacements are much lower than the roof values. The base displacements range from 0.075 cm to 2.0 cm, whereas the lateral roof displacements range between 1.625 cm to 8.635 cm for the same explosion. In other words, the horizontal displacements at the foundations are amplified from 4 to 16 multiples when it reaches the structure roof.
 - Under the same conditions, the vertical displacements are almost the same for the foundation and roof points. On the other hand, the vertical displacements due to the blast are almost 60% higher than the settlements that took place due to the structure loads.

- 2- In case of various charge weights; the response of structure is increased with increasing the charge weight at the same location in both vertical and horizontal directions. The structure is exposed to maximum base horizontal displacements of 3.87 cm, with respect to roof's lateral displacements, it is increased to a maximum of 14.14 cm. Thus, increasing the explosive charge weight has a slight effect on the structure horizontal displacements. About 70 multiples increase in the charge weight results only about 4 times the horizontal displacements. It should be noted that this case is related to blast waves passing through the foundation soils only, and do not account for air blast waves.
- 3- The structure's height and its flexibility have an effect on the structure response as the horizontal displacements at the foundations decreased with increasing the structure height. In contrary, the roof's lateral displacements increased with increasing the structure height. Increasing the structure height from 15.0 m to 30.0 m leads to an increase of roof lateral displacement up to 132.97 %. Although, the vertical displacement at the base is increased after the static analysis, they are decreased with decreasing the structure height due to the higher structure weight.
- 4- In all cases, the vibration of the structure is an instant spike reaching a maximum value just after detonation followed by decaying oscillations till the structure return to rest with permanent deformations. These permanent horizontal displacements and settlements are much higher in clays than those took place in sand.

6. REFERENCES

- [1] *ABAQUS Analysis Software*, (2011), "Software Suite for Finite Element Analysis and Computer-Aided Engineering", Version 6.11.
- [2] *Amini, M.*, (2013), "Blast Loading Effect on the Bearing Capacity of Shallow Foundations", *Journal of Advanced Defense Science and Technology*, Vol. 4, Number 3, pp. 199-209
- [3] *An, J., Tuan, C.Y., Cheeseman, B.A., and Gazonas, G.A.*, (2011), "Simulation of Soil Behavior under Blast Loading", *International Journal of Geomechanics*, Vol. 11, Issue 4, pp. 323-334
- [4] *Barnes, G.E.*, (2000), "Soil Mechanics: Principles and Practice", 2nd Edition, Palgrave, New York, ISBN 0-333-77776-X.
- [5] *Bulson, P.S.*, (1997), "Explosive Loading of Engineering Structures", 1st Edition, ENFN SPON Publishers, London, England.
- [6] *Chowdhury, H., and Wilt, T.E.*, (2015), "Characterizing Explosive Effects on Underground Structures", Center for Nuclear Waste Regulatory Analyses, Southwest Research Institute.
- [7] *Darke, J., and Little*, (1983), "Ground Shock from Penetrating Conventional Weapons" Proceedings of Symposium on Interaction of Non-Nuclear Munitions with Structures, U.S Air Force Academy, USA.
- [8] *Fiserova, D.*, (2006), "Numerical Analysis of Buried Mine Explosions with Emphasis on Effect of Soil Properties on Loading", Ph.D. Thesis, Cranfield University.
- [9] *Gamber, N.K.*, (2004), "Shallow Foundation Systems Response to Blast Load", M.Sc. Thesis, Ohio University.
- [10] *Hosseini, H., and Mohammad, A.*, (2015), "Assessment of Subsurface Explosion Caused by Tunnel Construction in Urban Areas", *JSEG Journal*, Vol. 5, Issue 2, pp. 45-49.
- [11] *Kanarachos, A., and Provatidis, C.*, (1998), "Determination of Buried Structure Loads Due to Blast Explosions", *Structures under Shock and Impact V*, Vol. 35, pp. 95-104.
- [12] *Lindsey, D.E.*, (1989), "An Investigation of Blasting Criteria for Structural and Ground Vibrations", M.Sc. Thesis, Ohio University.
- [13] *Rosengren, L., and Svedbjork, G.*, (1999), "Modeling of Ground-Shock Propagation in Soil Using FLAC" In *FLAC and Numerical in Geomechanics*, Vol. 21, pp. 401-405.
- [14] TM 5-855-1, (1986), "Fundamental of Protective Design for Conventional Weapons", Vicksburg, US Army Engineers Waterways Experimental Station, 1986.
- [15] *Wu, C., and Hao, H.*, (2004), "Modeling of Simultaneous Ground Shock and Air Blast Pressure on Nearby Structures from Surface Explosions", *International Journal of Impact Engineering*, Vol. 31, Issue 6, pp. 699-717.
- [16] *Xuansheng, C., Wei, J., and Jiexuan, M.*, (2014), "Dynamic Response of Concrete Frame Structure under a Blasting Demolition Environment", *EJGE Journal*, Vol. 19, pp. 823-837.
- [17] *Yang, Z.*, (1997), "Finite Element Simulation of Response of Buried Shelters to Blast Loadings", *Finite Elements in Analysis and Design*, Vol. 24, Issue 3, pp. 113-132.